RNA (1997), 3:498-513. Cambridge University Press. Printed in the USA.

Visualizing nuclear export of different classes of RNA by electron microscopy

NELLY PANTÉ,[1] ARTUR JARMOLOWSKI,[2,3] ELISA IZAURRALDE,[2,4] URSULA SAUDER,[1] WERNER BASCHONG,[1] and IAIN W. MATTAJ[2]

[1]M.E. Müller Institute for Microscopy, Biozentrum, University of Basel, Klingelbergstrasse 70, CH-4056 Basel, Switzerland
[2]European Molecular Biology Laboratory, Meyerhofstrasse 1, D-69117 Heidelberg, Germany

ABSTRACT

Export of RNA from the cell nucleus to the cytoplasm occurs through nuclear pore complexes (NPCs). To examine nuclear export of RNA, we have gold-labeled different types of RNA (i.e., mRNA, tRNA, U snRNAs), and followed their export by electron microscopy (EM) after their microinjection into *Xenopus* oocyte nuclei. By changing the polarity of the negatively charged colloidal gold, complexes with mRNA, tRNA, and U1 snRNA can be formed efficiently, and gold-tagged RNAs are exported to the cytoplasm with kinetics and specific saturation behavior similar to that of unlabeled RNAs. U6 snRNA conjugates, in contrast, remain in the nucleus, as does naked U6 snRNA. During export, RNA–gold was found distributed along the central axis of the NPC, within the nuclear basket, or accumulated at the nuclear and cytoplasmic periphery of the central gated channel, but not associated with the cytoplasmic fibrils. In an attempt to identify the initial NPC docking site(s) for RNA, we have explored various conditions that either yield docking of import ligands to the NPC or inhibit the export of nuclear RNAs. Surprisingly, we failed to observe docking of RNA destined for export at the nuclear periphery of the NPC under any of these conditions. Instead, each condition in which export of any of the RNA–gold conjugates was inhibited caused accumulation of gold particles scattered uniformly throughout the nucleoplasm. These results point to the existence of steps in export involving mobilization of the export substrate from the nucleoplasm to the NPC.

Keywords: colloidal gold; gold-tagged RNAs; nuclear pore complex; *Xenopus* oocyte microinjection

INTRODUCTION

Bidirectional molecular trafficking between the cytoplasm and the cell nucleus occurs through the nuclear pore complexes (NPCs), ~125-MDa supramolecular assemblies embedded in the double-membraned nuclear envelope (reviewed by Davis, 1995; Panté & Aebi, 1996a). The NPC allows passive diffusion of ions and small molecules through aqueous channels with a physical diameter of ~9 nm, and mediates active transport of both proteins and RNAs as ribonucleoprotein (RNP) particles. The active transport is highly selective, energy- and temperature-dependent, and is mediated by several cellular factors. The transport ligands are recognized by saturable receptors (reviewed by Melchior & Gerace, 1995; Görlich & Mattaj, 1996; Panté & Aebi, 1996b). The complex of transport ligand and cellular factors is then targeted to the NPC, and it is translocated actively through the central gated channel of the NPC (also called central plug or transporter). Import of the majority of nuclear proteins involves recognition of short stretches of basic amino acids called nuclear localization sequences (NLSs; reviewed by Dingwall & Laskey, 1991; Garcia-Bustos et al., 1991; Boulikas, 1993), whereas incompletely defined signals mediate nuclear import of snRNPs (reviewed in Lührmann et al., 1990; Izaurralde & Mattaj, 1992) and of some nuclear glycoproteins (Duverger et al., 1995). In contrast, the NLS of the heterogeneous nuclear RNP (hnRNP) A1 protein comprises a 38-amino acid region termed M9, which is also found in a few closely related hnRNP proteins (Michael et al., 1995; Siomi & Dreyfuss, 1995; Weighardt et al., 1995). Nuclear export of RNAs is also a signal-mediated process. Because most RNAs are associated with proteins in the nucleus and are transported through the NPC as RNP particles (Mehlin et al., 1995; reviewed by Izaurralde & Mattaj,

Reprint requests to: Nelly Panté, M.E. Müller Institute for Microscopy, Biozentrum, University of Basel, Klingelbergstrasse 70, CH-4056 Basel, Switzerland; e-mail: pante@ubaclu.unibas.ch.
[3]Present address: Institute of Molecular Biology and Biotechnology, Department of Biopolymer Biochemistry, Miedzychodzka 5, 60371 Poznan, Poland.
[4]Present address: University of Geneva, Department of Molecular Biology, Quai Ernest Ansermet 30, 1211 Geneva 4, Switzerland.

1995), it was initially unclear whether the nuclear export signal resided on the RNA, on the RNA-binding proteins, or on both. The first nuclear export signals, called NESs, have now been identified on various proteins, including the HIV-1 Rev protein (Fischer et al., 1995), the heat-stable protein kinase inhibitor (PKI; Wen et al., 1995), the RNA polymerase III transcription factor TFIIIA (Fridell et al., 1996), and the hnRNP A1 protein (Michael et al., 1995). The first three NESs are short leucine-rich stretches of amino acids, and a consensus sequence for this class of NESs has been defined (Bogerd et al., 1996). The NES of hnRNP A1 is apparently identical to, or at least overlaps with, the M9 NLS signal (Michael et al., 1995).

The finding that such different signals are capable of directing active export from the nucleus suggests the existence of distinct export pathways. Moreover, competition studies between different classes of RNAs have demonstrated that each type of RNA can competitively inhibit export of RNAs from the same class without affecting the export of the other types of RNA (Jarmolowski et al., 1994; Pokrywka & Goldfarb, 1995). Thus, the export of each class of RNA from the nucleus is probably, at least in part, mediated by distinct factors. Consistent with this, saturation of the Rev NES pathway prevents the export of U snRNAs and 5S rRNA, whereas saturating amounts of hnRNP A1 specifically inhibit mRNA export (Fischer et al., 1995; Izaurralde et al., 1997). Recently, proteins involved in nuclear export of two different exported RNAs have been identified. First, the HIV-1 Rev protein was shown to affect the export of pre-mRNAs directly or other RNAs containing its binding site, the Rev Response Element (Malim & Cullen, 1993; Fischer et al., 1994, 1995). Second, a nuclear cap-binding protein complex (CBC) that mediates export of U snRNAs was identified. U snRNA primary transcripts carry monomethylated cap structures that have a role in their nuclear export (Hamm & Mattaj, 1990; Izaurralde et al., 1992). More recently, a CBC composed of two cap-binding proteins, CBP20 and CBP80, was purified (Izaurralde et al., 1994) and shown to mediate the export of U snRNAs (Izaurralde et al., 1995). CBC has also been found associated with Balbiani Ring (BR) messenger RNP particles during their nuclear export (Visa et al., 1996b).

The cellular factors mediating the different export pathways are not yet defined, although it is probable that some of the same cellular factors involved in nuclear import of NLS proteins, particularly the small GTPase Ran/TC4, might also be involved in at least some of the nuclear export pathways (reviewed by Izaurralde & Mattaj, 1995; Koepp & Silver, 1996). Candidate mediators of the M9 pathway (Pollard et al., 1996) and the Rev-NES pathway (Bogerd et al., 1995; Fritz et al., 1995; Stutz et al., 1995) have also been identified. The candidate factors in the case of Rev, human RIP/Rab and yeast RIP, were identified in yeast two-hybrid screens by their interaction with the Rev activation domain, a region of the protein that plays an essential role in Rev-mediated export (Bogerd et al., 1995; Fritz et al., 1995; Stutz et al., 1995). These proteins resemble nucleoporins, and indeed several nucleoporins, more specifically repeat regions from these proteins, also show positive interaction with either human RIP/Rab or yeast Rip in the two-hybrid assay (Stutz et al., 1995, 1996; Fritz & Green, 1996). Injection of these repeats into the nucleus of *Xenopus* oocytes, like the injection of saturating amounts of NES peptide conjugates, causes specific inhibition of export of certain RNAs (Fischer et al., 1995; Stutz et al., 1996).

In contrast to the progress toward characterizing soluble transport factors, little is known about the structural events of nuclear export. Because the NPC is a highly organized assembly with a distinct 3D architecture (Hinshaw et al., 1992; Akey & Radermacher, 1993), understanding the mechanism of nuclear export will require not only the identification of cellular factors mediating the different export pathways, but identification of steps followed by the export ligand during its transport through the NPC. For nuclear import of NLS proteins, which is the best characterized nuclear transport process, three different transport intermediates arrested at the NPC have been visualized by electron microscopy (EM). One is at the distal part of the cytoplasmic fibrils of the NPC, which is visualized when import is inhibited by the lectin wheat germ agglutinin (WGA), or when import ligands are injected close to the nuclear envelope (Newmeyer & Forbes, 1988; Richardson et al., 1988; Panté & Aebi, 1996c). WGA binds to nucleoporins that contain O-linked N-acetylglucosamine residues (Snow et al., 1987) and appears to "plug" the cytoplasmic opening of the central pore so that the import ligand is arrested at the initial docking site at the cytoplasmic fibrils (Panté & Aebi, 1996c). The second import intermediate is observed at the cytoplasmic entry to the central gated channel when nuclear import is attenuated by chilling (Panté & Aebi, 1996c). Finally, a third import-arrested intermediate has been visualized at the nuclear side of the NPC, probably associated with the NPC nuclear fibrils (i.e., the nuclear basket) when a mutant importin β (the large subunit of the nuclear protein import receptor) deficient in Ran binding was used (Görlich et al., 1996c).

By analogy with NLS protein import, RNAs destined for export might first bind to the nuclear baskets. From this initial docking site, the export ligand might then be delivered to the nuclear entry to the central gated channel and subsequently translocated to the cytoplasm. Studies of the nuclear export of the giant BR RNP particles of *Chironomus tentans* support this view (Mehlin et al., 1992, 1995; Kiseleva et al., 1996). To visualize these hypothetical steps of nuclear export for smaller RNA export ligands, we have developed a pro-

tocol to conjugate RNAs to colloidal gold. The gold-tagged RNAs were then microinjected into the nuclei of *Xenopus* oocytes and the fate of the RNA-gold particles during their nuclear export was followed by EM. Similar experiments conducted previously led to the conclusion that gold conjugates carrying either tRNA, 5S rRNA, or poly A were all exported similarly (Dworetzky & Feldherr, 1988). This was not expected because tRNA and 5S rRNA show a difference of roughly 50-fold in export rate when not conjugated to gold (Zasloff, 1983; Guddat et al., 1990; Jarmolowski et al., 1994). In addition, in these earlier studies, only about 5% of the RNA conjugates were ever exported, indicating that either the conjugates were unstable, or the RNA ligand was not accessible to export factors on the surface of the gold particles. The new methodology developed here allows relatively efficient nuclear export of the RNA-gold conjugates (70% or more) and the conjugates are exported with characteristics similar to the naked RNAs. We have used this method to study steps in the export of various classes of microinjected RNA export ligands.

RESULTS

Direct conjugation of recombinant RNAs to colloidal gold

In order to visualize nuclear export of various types of RNA by EM, we first developed an efficient procedure to conjugate RNAs directly to colloidal gold. Colloidal gold is usually formed by reduction of gold chloride into negatively charged particles that can be coupled directly to proteins such as lectins, protein A, and antibodies by noncovalent electrostatic adsorption. This standard procedure has been used extensively in immunoelectron microscopy (see e.g., Verkleij & Leunissen, 1990). However, this method did not yield gold complexes reproducibly with nucleic acids in our hands, perhaps not surprisingly given the high overall negative charge of these macromolecules. By changing the charge of the gold colloids with $Th(NO_3)_4$, we have, however, been able to successfully conjugate several in vitro-synthesized RNAs including tRNA, U1 ΔSmRNA, U6 ΔssRNA, and the mRNA coding for dihydrofolate reductase (DHFR-mRNA) to colloidal gold with high yield of conjugates. To confirm that the RNA-gold complexes made by this method contained RNA, two different approaches were taken: (1) coupling [^{32}P]RNAs to positively charged gold colloids; and (2) releasing the RNA from the RNA-gold complex by freezing and thawing. With the first approach, we always obtained radiolabeled RNA-gold complexes, whereas, by the second approach, the RNA was released into solution as revealed by ethidium bromide staining. These results indicated that the RNAs were indeed coupled to positively charged colloidal gold.

Nuclear export of gold-labeled RNAs

Next we wanted to find out whether the RNA-gold complexes prepared by our procedure are exported from the nucleus. For this purpose, ^{32}P-labeled DHFR-mRNA, tRNA, and U1 ΔSmRNA were coupled with positively charged colloidal gold using the same procedure as for cold RNAs. The resulting [^{32}P]-labeled RNA-gold complexes were then microinjected into *Xenopus* oocyte nuclei, and the appearance of radioactivity in the cytoplasm was monitored after incubation at room temperature for different time periods. As documented in Table 1, immediately after their nuclear injection, the great majority of all three gold-labeled [^{32}P]RNAs tested were found in the nuclear fraction. After further incubation, the cytoplasmic fraction contained progressively more radioactivity up to a certain time point, and the appearance of radioactivity in the cytoplasm plateaued at different times for the various conjugates. In experiments where the same RNAs were microinjected in the nonconjugated form [data not shown, but see Jarmolowski et al. (1994), who reported identical results], export of DHFR-mRNA or U1 ΔSmRNA followed similar kinetics, with a lag phase of roughly 20 min followed by export of roughly half the injected RNA over a period of the next 30–40 min and of most of the rest of the RNA over the next hour, whereas tRNA was exported more rapidly, with a half-time of roughly 10 min. Microinjected RNA-gold complexes were exported to the cytoplasm with roughly similar kinetics (Table 1). However, even after 6 h of incubation at room temperature, we always detected radioactivity in the nuclear fraction for all three [^{32}P]RNA-gold complexes tested. Thus, the nuclear export of RNA-gold was incomplete. However, in contrast to a similar previous study, where only approximately 5% of injected RNA conjugates were exported (Dworetzky & Feldherr, 1988), under the conditions used here roughly 70% of the RNA-gold was exported

TABLE 1. Export rate of RNA-gold conjugates.[a]

Time after injection (min)	tRNA	U1 ΔSmRNA	mRNA
0	17	15	12
15	38	ND[b]	ND
30	70	ND	ND
60	74	45	35
240	ND	66	72
360	ND	68	78
60[c]	12	ND	ND
240[c]	ND	11	9

[a] Values are the % of the ^{32}P cpm in the cytoplasmic fraction of dissected oocytes. For each time point, 10 oocytes were microinjected and dissected. Data presented are average from two experiments.

[b] ND, not determined.

[c] Oocytes kept at 4 °C after microinjection.

to the cytoplasm (Table 1). Export of all three RNA-gold conjugates was energy dependent, because it was prevented by cooling the oocytes (Table 1).

Visualization of the route of nuclear export

To visualize the export of RNA through NPCs, we then microinjected *Xenopus* oocyte nuclei with RNA-gold complexes and prepared the injected oocytes for embedding and thin-section EM at different times after microinjection. Again, DHFR-mRNA, tRNA, and U1 ΔSmRNA were used. In Figure 1, typical results of the nuclear export of these RNA-gold conjugates are shown. Times of embedding were chosen so as to allow observation of the conjugates associated with NPCs, but should not be mistaken for time courses of export of the conjugates. Thus, for example, for DHFR-mRNA, where export plateaued roughly 3–4 h after microinjection, the samples were processed for embedding and thin-section EM 0 min, 45 min, 1.5 h, and 2.5 h after microinjection. For all samples, single gold particles as well as aggregates of two, three, and more gold particles were found in the nucleoplasm at all time points (Fig. 1). Because uncoupled positively charged gold colloids appeared as single particles in the EM, the number of gold particles per RNA molecule in the RNA-gold complexes was variable, with about 64% and 20% RNA molecule coupled with one and two gold particles, respectively (independent of the type of RNA). RNA-gold complexes with only one gold particle per RNA molecule could have been purified (e.g., by gradient centrifugation), but this would have required prohibitively large quantities of recombinant RNA. Thus, we performed the export experiments with the heterogeneous RNA-gold complexes containing variable numbers of gold particles per RNA. Upon microinjection into *Xenopus* oocyte nuclei, only RNA complexed with one or two gold particles was ever found associated with NPCs or exported to the cytoplasm, whereas bigger gold aggregates remained in the nucleoplasm (see Fig. 1). This is a likely explanation of the result obtained with [^{32}P]RNA-gold (see above and Table 1), which indicated that only about 70% of the RNA-gold was exported to the cytoplasm.

Immediately after injection into the nucleus, the RNA-gold particles were distributed randomly throughout the nucleoplasm (Fig. 1, arrows in all three parts). After varying times of incubation at room temperature, dependent on the identity of the coupled RNA, RNA-gold complexes containing one or two gold particles were found associated with NPCs (Fig. 1B, arrowheads in all three parts), and progressively also in the cytoplasm (Fig. 1C,D, small arrows in all three parts). In contrast, when gold-conjugated U6 ΔssRNA—an RNA that is not exported to the cytoplasm (Vankan et al., 1990)—was microinjected into *Xenopus* oocyte nuclei, the U6 ΔssRNA-gold particles were distributed evenly throughout the nucleoplasm even after 6 h of incubation at room temperature (Fig. 2). Thus, the specificity and kinetics of export of the different gold-RNA conjugates resembled those of unconjugated RNAs.

Export of RNA–gold conjugates is specifically competed

Previous work has shown that export of mRNA, U snRNA, or tRNA from the nucleus is a saturable process that is inhibited by an excess of an RNA of the same class, but not by other types of RNA (Jarmolowski et al., 1994). This provided an additional test of whether the RNA-gold conjugates behaved like nonconjugated RNAs. When a saturating amount of unconjugated mRNA was microinjected into *Xenopus* oocyte nuclei before microinjection of mRNA-gold, the gold particles remained randomly distributed throughout the nucleoplasm, and hence did not associate with NPCs and were not exported (Fig. 3B, arrows; see also Table 2), even 4 h after microinjection. In contrast, when a similar amount of unlabeled tRNA or U1 ΔSmRNA was microinjected before mRNA-gold, the mRNA-gold particles were targeted to the NPC and exported to the cytoplasm (Fig. 3C,D). As documented in Table 2, quantitation of NPCs with associated gold particles revealed that, 45 min after microinjection, about 40% of the NPCs contain mRNA-gold particles for both the control experiment, where mRNA-gold was microinjected alone, and the competition experiments, where unlabeled tRNA or U1 ΔSmRNA were pre-injected before mRNA-gold. Thus, we have confirmed by direct visualization using EM that tRNA or U1 ΔSmRNA have little or no effect in the nuclear export of mRNA-gold.

Analogous results were obtained when the competition studies were performed using tRNA-gold or U1 ΔSmRNA-gold instead of mRNA-gold, confirming the results of Jarmolowski et al. (1994), that each type of RNA competitively inhibited its own export, but not the export of other types of RNAs. Moreover, as illustrated for the inhibition of mRNA-gold by unlabeled mRNA (Fig. 3B), the RNA-gold particles of all three types remained in the nucleoplasm when export was

TABLE 2. Percentage of NPCs decorated with mRNA-gold particles in competition studies between mRNA-gold and unlabeled RNAs.[a]

	NPCs decorated with gold
mRNA-gold	41.2%
mRNA + mRNA-gold	0%
tRNA + mRNA-gold	39.6%
U1 ΔSmRNA + mRNA-gold	42.2%

[a]Competition experiments were done as described in Figure 3. Eighty NPCs were evaluated for each condition.

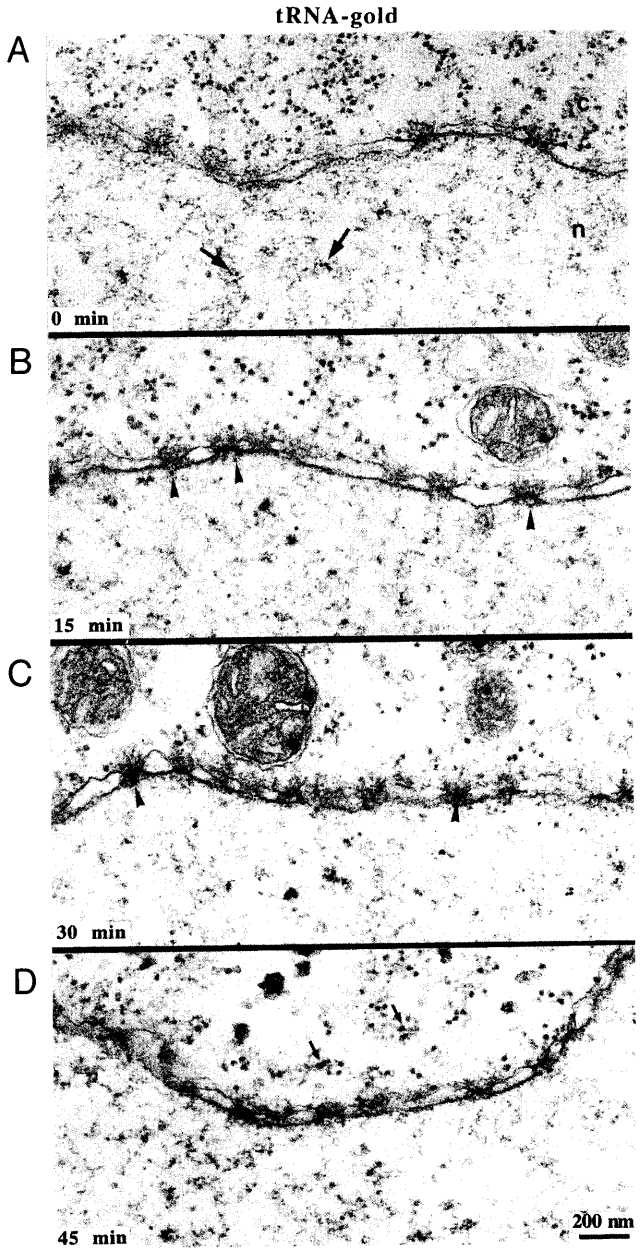

FIGURE 1. Visualization of nuclear export of tRNA-gold, U1 ΔSmRNA-gold, and DHFR mRNA-gold through the NPC. The three RNAs coupled with positively charged colloidal gold particles (8-nm diameter) were microinjected into the nucleus of *Xenopus* oocytes, and the samples were processed for embedding and thin-section EM after: Part I (**A**) 0 min, (**B**) 15 min, (**C**) 30 min, and (**D**) 45 min of incubation for tRNA; Part II (**A**) 0 min, (**B**) 30 min, (**C**) 1 h, and (**D**) 1.5 h for U1 ΔSmRNA; and Part III (**A**) 0 min, (**B**) 45 min, (**C**) 1.5 h, and (**D**) 2.5 h for mRNA gold. Shown are views along cross-sectioned *Xenopus* oocyte nuclear envelopes. Arrows in the A panels point to gold particles in the nucleus immediately after microinjection. Arrowheads in the B, C, and D panels mark gold particles associated with NPCs, whereas the small arrows in the C and D panels point to gold particles that have been exported to the cytoplasm. c, cytoplasmic side of the NE; n, nuclear side of the NE. Scale bar, 200 nm. (*Figure continues on facing page.*)

saturated and did not associate detectably with the nucleoplasmic face of the NPC (data not shown). We conclude that the limiting factors for export of each RNA class must reside in the nucleoplasm and not at the NPC.

RNA moves through the center of NPCs

By quantitation of the position and distribution of gold particles coupled to the *Xenopus* nuclear protein nucleoplasmin during nuclear import, two distinct cytoplasmic NPC binding regions for import ligands have been identified (Panté & Aebi, 1996c). Similarly, we have evaluated the position and distribution of mRNA-gold particles associated with NPCs in cross-sectioned nuclear envelope. This type of analysis should reveal the position of rate-limiting events in RNA nuclear export. As shown in Figure 4, at each time point, the gold particles were found associated with both the nuclear and cytoplasmic side of the NPC and predominantly distributed along the central axis of the NPC. The amount of RNA-gold particles on the nuclear side was initially high and decreased with time, whereas the number of RNA-gold particles on the cytoplasmic side increased with time. This is a consequence of the reduction in number of transportable RNA-gold conjugates remaining in the nucleus at increasing times after microinjection. On the nuclear side of the NPC, gold particles were found at variable vertical distances (i.e., the distance perpendicular to the central plane of

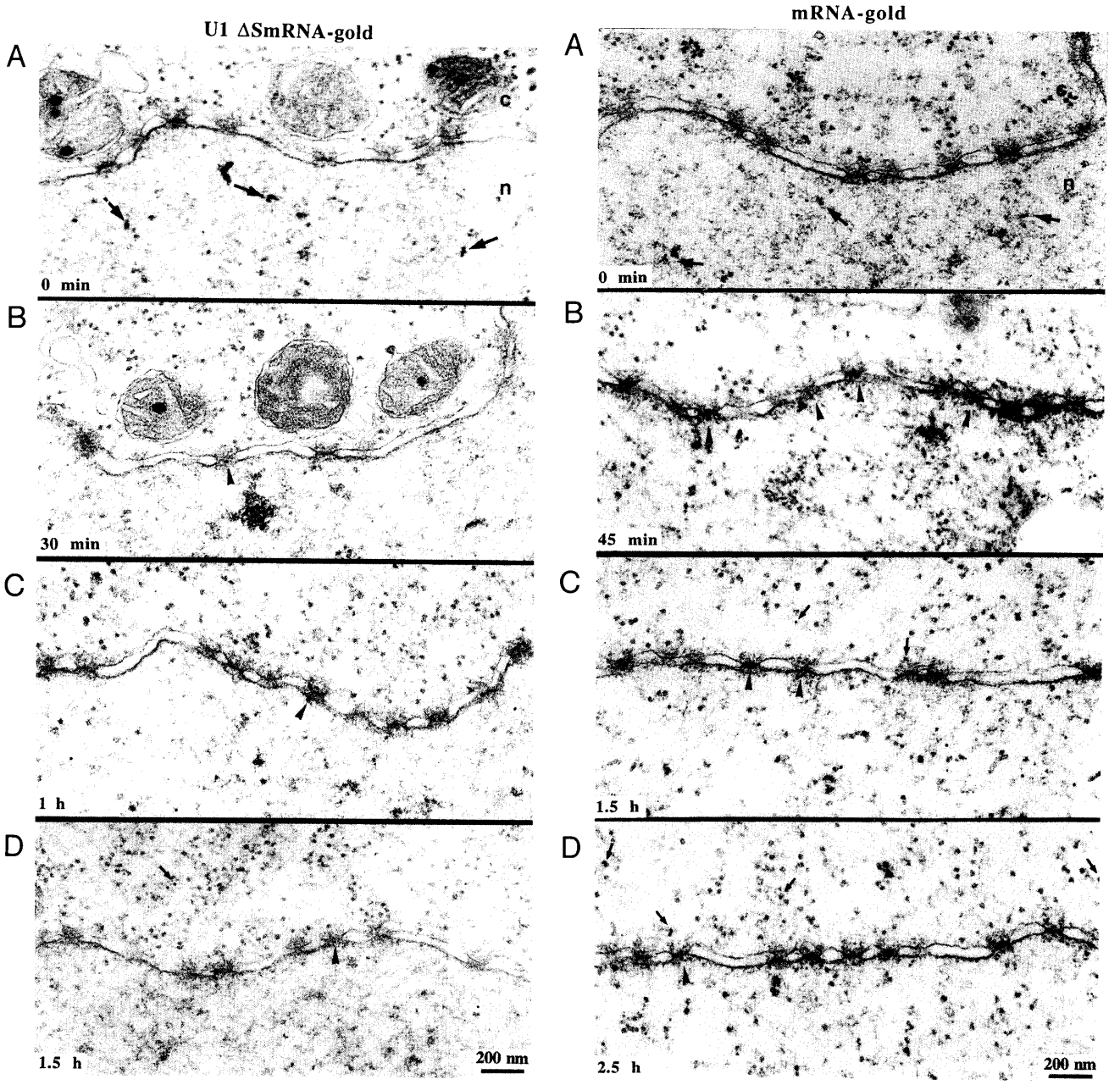

FIGURE 1. *Continued.*

the NE) of up to ~50 nm. As illustrated in Figure 5A, this position corresponds to RNA-gold particles associated with the nuclear basket of the NPC. Very strikingly, gold particles were not found at vertical distances between −10 nm and +10 nm. Instead, RNA-gold conjugates appear to accumulate at the nuclear and cytoplasmic periphery of the central gated channel of the NPC (Fig. 5B,C). Taken together, the results of the quantitative analysis indicate that once the export ligand reaches the cytoplasmic face of the NPC, it is released into the cytoplasm without binding to the short kinky fibrils emanating from the cytoplasmic periphery of the NPC, and that translocation of the export ligand complex across the central gated channel occurs very quickly.

Export ligands do not accumulate at the NPC at low temperature or in the presence of WGA

The import of nuclear proteins can be divided into two steps. An energy-independent event, where the nuclear protein-import receptor complex docks to the NPC, and the energy-requiring translocation through the NPC. Accumulation of import ligand at the NPC cytoplasmic fibrils and at the cytoplasmic periphery of the NPC central gated channel have been observed by

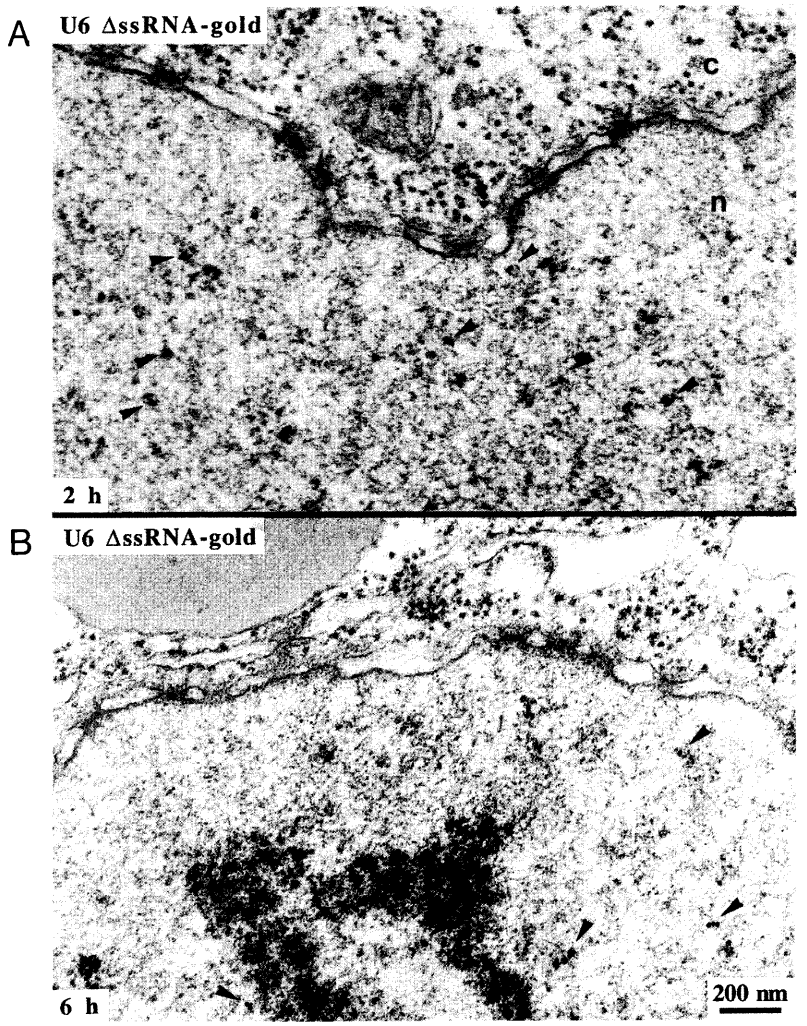

FIGURE 2. U6 ΔssRNA-gold conjugates are not exported to the cytoplasm. U6 ΔssRNA-gold complexes were microinjected into the nucleus of *Xenopus* oocytes, and the samples were processed for embedding and thin-section EM after (**A**) 2 h, and (**B**) 6 h of incubation at room temperature. The U6 ΔssRNA-gold particles remained randomly distributed throughout the nucleoplasm at both time points (arrowheads). c, cytoplasmic side of the NE; n, nuclear side of the NE. Scale bar, 200 nm.

EM when nuclear import is inhibited by the presence of WGA and at 4 °C, respectively (Newmeyer & Forbes, 1988; Richardson et al., 1988; Panté & Aebi, 1996c). We have used the same conditions in an attempt to identify the initial NPC docking site(s) for the various RNA export ligands. As has been shown previously by Dworetzky and Feldherr (1988), when oocytes were kept at 4 °C after nuclear microinjection of mRNA-gold, both NPC association and export of mRNA-gold was clearly inhibited (Fig. 6). The mRNA-gold particles were distributed randomly throughout the nucleoplasm and not associated with NPCs even after 6 h of incubation at 4 °C (Fig. 6B,C, arrows). Similar results were obtained with the other tRNA-gold and U1 ΔSmRNA-gold conjugates (data not shown).

Our results suggested that chilling the oocytes inhibited early steps of the RNA export pathway that occur in the nucleoplasm. Injection experiments using WGA to inhibit U snRNA or tRNA export showed similar results (data not shown). To address this question further, we explored the inhibition of WGA by using WGA conjugated with colloidal gold. As has been shown previously (Panté & Aebi, 1996c), cytoplasmic microinjection of WGA-gold "plugs" the cytoplasmic entry to the central pore channel (Fig. 7A, arrowheads). However, when microinjected into the nucleus, WGA-gold accumulated at the nuclear periphery of the NPC to variable distances of up to ~60 nm from the NPC central plane (Fig. 7B, arrowheads). Thus, WGA not only appears to "plug" the nuclear entry of the central pore channel, but it also accumulates within the nuclear baskets. Similar to the inhibition of export of U1 ΔSmRNA-gold by cytoplasmic or nuclear microinjection of unlabeled WGA, when 14-nm WGA-gold was microinjected into the cytoplasm or into the nucleus of *Xenopus* oocytes 1 h prior to nuclear microinjection of 8-nm U1 ΔSmRNA-gold, the 8-nm gold particles remained dispersed within the nucleoplasm and did not associate with the nuclear periphery of NPCs (Fig. 7C,D, arrows). Because the WGA was pre-injected, it is possible that sites on the nuclear face of the NPC are saturated by endogenous RNPs whose export is blocked before we introduce the RNA-gold conjugates. However, we note that docked import substrates were observable even after WGA pre-injection into the cytoplasm in the studies of protein import.

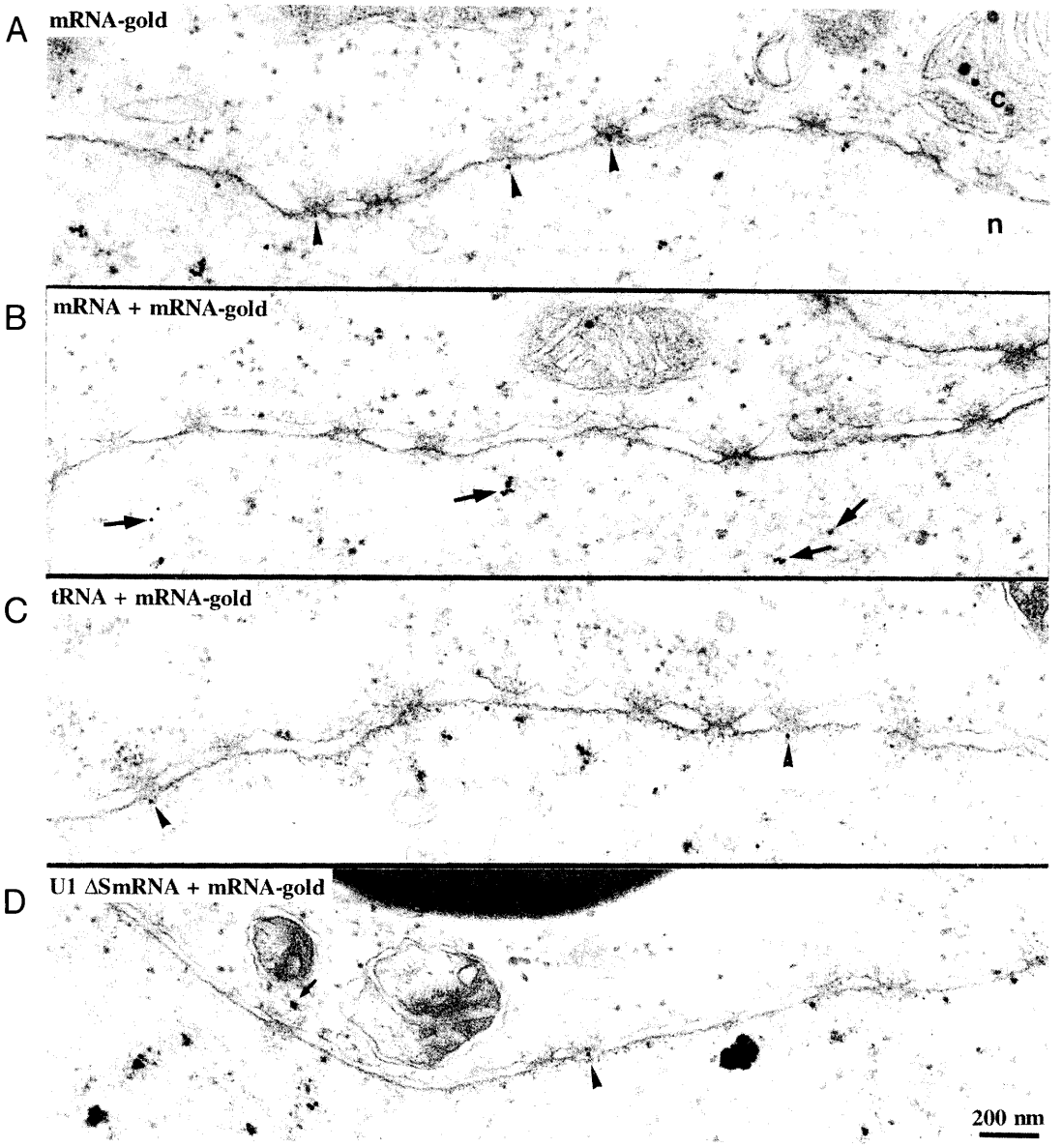

FIGURE 3. Competition experiments between mRNA-gold and unlabeled RNAs. DHFR mRNA-gold conjugates were injected either alone (**A**) or 1 h after nuclear injection of saturating amounts of unlabeled mRNA (**B**), tRNA (**C**), or U1 ΔSmRNA (**D**) into the nucleus of *Xenopus* oocytes. Gold particles were found associated with NPCs and in the cytoplasm for oocytes microinjected without competitor (A) with unlabeled tRNA (C), and unlabeled U1 ΔSmRNA (D), some of which are marked with arrowheads. In contrast, when the oocytes were pre-injected with unlabeled mRNA in their nucleus, the gold particles remained in the nucleoplasm (B, arrows). Samples were processed for embedding and thin-section EM 45 min after injection of mRNA-gold. Incubation was at room temperature. c, cytoplasmic side of the NE; n, nuclear side of the NE. Scale bar, 200 nm.

Effect of the importin β binding (IBB) domain of importin α and hnRNP A1 on nuclear export of RNAs

Because saturation of each RNA export pathway, chilling, or the presence of WGA all had the same effect on the distribution of nuclear RNA-gold conjugates microinjected into the nucleus, we decided to examine the effects of two known inhibitors of RNA export that are specific for particular types of RNA. The IBB domain of importin α competitively inhibits NLS-mediated nuclear protein import and also specifically blocks U snRNA export (Görlich et al., 1996a, 1996b; Weis et al., 1996), whereas saturating amounts of hnRNP A1 protein prevents mRNA export without affecting other RNAs (Izaurralde et al., 1997).

An IBB domain-protein A fusion protein was therefore microinjected into the cytoplasm of *Xenopus* oocytes 1 h before nuclear microinjection of U1 ΔSmRNA- or DHFR mRNA-gold conjugates. As illustrated in Figure 8A and B, the U1 ΔSmRNA-gold particles remained dispersed within the nucleoplasm and did not

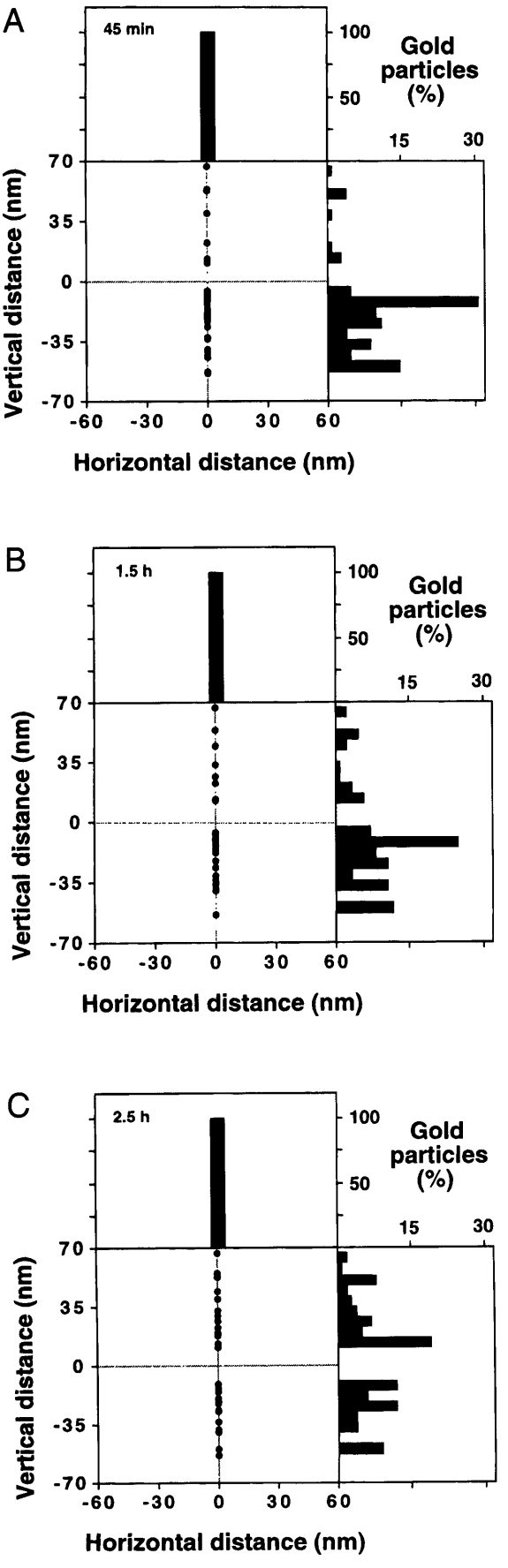

associate with NPCs in the presence of the IBB fusion protein, whereas mRNA-gold was exported normally. Thus, IBB domain injection inhibited an early step(s) of the export pathway of U1 ΔSmRNA.

When hnRNP A1 was pre-injected into *Xenopus* oocyte nuclei before nuclear microinjection of mRNA-gold conjugates, it inhibited their export efficiently and retained them in the nucleoplasm without association with the nuclear periphery of the NPCs (Fig. 8D, arrows). In contrast, hnRNP A1 had no effect on U1 ΔSmRNA-gold export (Fig. 8C, arrowheads). Again, this inhibition led to the accumulation of mRNA-gold conjugates in the nucleoplasm, and not at the NPC.

DISCUSSION

Previous work had shown that, upon microinjection of tRNA, 5SRNA, or homopolymeric RNA conjugated to colloidal gold particles into *Xenopus* oocyte nuclei, the RNA-gold particles are translocated to the cytoplasm through the NPCs (Dworetzky & Feldherr, 1988). More recently, several biochemical studies have provided further insight into RNA export (reviewed by Izaurralde & Mattaj, 1995; Fischer et al., 1996; Görlich & Mattaj, 1996). Thus, for example, the kinetics of nuclear export of different types of RNA is now better characterized (e.g., Jarmolowski et al., 1994; Pokrywka & Goldfarb, 1995). Several conditions and inhibitors that influence nuclear export have been defined (e.g., Featherstone et al., 1988; Neuman de Vegvar & Dahlberg, 1990; Jarmolowski et al., 1994; Görlich et al., 1996b; Izaurralde et al., 1997), and nuclear localization signals (NESs) and cellular factors mediating nuclear export have been identified (reviewed by Gerace, 1995; Fischer et al., 1996; Görlich & Mattaj, 1996). However, the molecular details of the mechanisms underlying RNA export remain largely unknown. In this study, we have extended the work of Dworetzky and Feldherr (1988) to visualize nuclear export of different classes of colloidal gold-RNA conjugates and to dissect nuclear export into distinct steps. In addition, we have demonstrated

FIGURE 4. Analysis of the position and distribution of mRNA-gold associated with NPCs. The position of gold particles, which is defined by horizontal distance (i.e., the distance from the central axis of the NPC perpendicular to the nuclear envelope) and vertical distance (i.e., the distance perpendicular to the central plane of the nuclear envelope) was measured in cross-sectioned nuclear envelopes (as in Fig. 1) and plotted in a single dot graphic. Due to the lack of resolution, each dot may represent several gold particles. Histograms for the distribution of gold particles for horizontal and vertical distances are shown on adjacent panels. Samples prepared for EM (**A**) 45 min, (**B**) 1.5 h, and (**C**) 2.5 h after microinjecting the oocyte nuclei with 8-nm mRNA-gold were analyzed. Distribution for the vertical distances was variable with time, whereas distribution for the horizontal distance always yielded a single major peak corresponding to the center of the NPC. Cross-sectioned nuclear envelopes from four different experiments were analyzed, which yielded 100, 83, and 98 particles for A, B, and C, respectively.

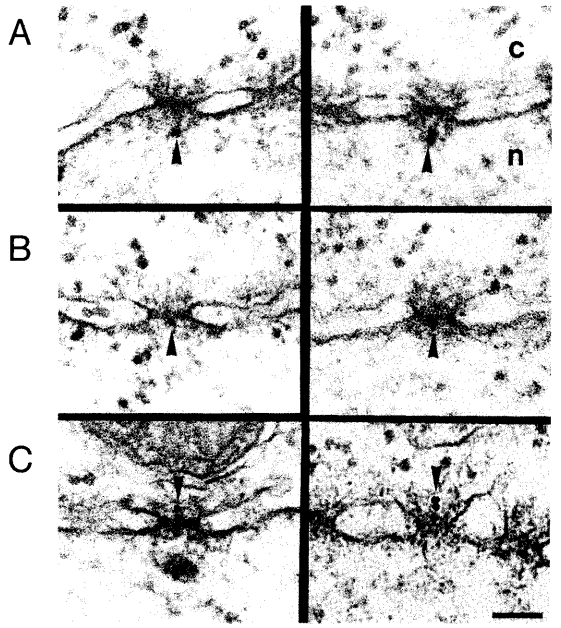

FIGURE 5. Gallery of selected examples of NPC cross-sections revealing mRNA-gold particles associated with the NPC. At the nuclear side of the NPC, mRNA-gold particles were found up to a vertical distance of 50 nm from the NPC central plane, which corresponds to the position of the nuclear basket (**A**). As revealed by the quantitative analysis (Fig. 4), RNA-gold particles accumulated at vertical distance of −15 nm and +15 nm, which represent RNA-gold associated with the nuclear (**B**) and cytoplasmic (**C**) periphery of the NPC central gated channel. c, cytoplasmic side of the NE; n, nuclear side of the NE. Scale bar, 100 nm.

that these gold conjugates behave similarly to naked RNA with respect to nuclear export and explored conditions known to block RNA export in order to yield transport intermediates arrested at the NPC.

Because in vitro-produced RNAs could not be coupled to negatively charged colloidal gold particles by standard procedures, we first developed a method to change the charge of the gold colloids. Several recombinant RNAs, including mRNA, tRNA, and U snRNAs, were coupled successfully to positively charged colloidal gold particles, and the resulting RNA-gold complexes were exported to the cytoplasm after their microinjection into *Xenopus* oocyte nuclei.

In order to visualize export intermediates arrested at stages of nuclear export, we have employed conditions known to inhibit export of most RNAs (i.e., low temperature, inhibition by injection of WGA, competition with saturable amounts of RNA). Very strikingly, none of these conditions caused the export ligands to accumulate at or near the NPC. By quantitation of RNA-gold particles associated with NPCs during their nuclear export, we have, however, observed RNA-gold particles within the nuclear basket, and associated with both the nuclear and cytoplasmic periphery of the central gated channel. From our data, we cannot distinguish whether the export ligand sequentially associates first to the nuclear baskets and then to the nuclear periphery of the central gated channel. Because the distribution of RNA-gold particles at about −50 nm from the NPC central plane was always smaller than that at −15 nm, we speculate that, if RNA-gold binds sequentially to these two NPC regions, the delivery of the export ligand from the nuclear baskets to the central gated channel occurs very fast. Similarly, because gold particles were not observed within the central gated channel (i.e., for vertical distances between −10 and 10 nm), we conclude that the translocation of the export ligand through the NPC central gated channel occurs very quickly. These studies are in agreement with those of Daneholt and colleagues, who have performed detailed examination of the export of the giant BR RNPs from the nuclei of *C. tentans* salivary gland cells (Mehlin et al., 1992, 1995; Kiseleva et al., 1996; Visa et al., 1996a, 1996b). In these studies, BR RNPs are often seen docked at the nuclear basket structures, but are seen only rarely during the actual translocation step. Our studies with RNA conjugates containing much smaller RNAs (BR mRNAs are > 30 kb in length) suggest that the "unpackaging" of BR RNPs that is required for their export does not introduce a new rate-limiting step in export, but rather that all substrates will pause at the basket structures and on the nuclear entry to the central gated channel before translocation occurs. This does not, of course, mean that a very large RNP like the BR RNP might not require a considerably longer time to pass this step. For example, if removal of nuclear proteins is part of this step, this may require longer time if the RNP is larger.

The binding of the RNA-gold particles to these three NPC regions might involve interactions of the export ligand with NPC proteins (nucleoporins). That nucleoporins have a role in nuclear export has been suggested by inhibition of nuclear export by (1) antinucleoporin antibodies, and (2) the lectin WGA (Featherstone et al., 1988; Bataillé et al., 1990; Neuman de Vegvar & Dahlberg, 1990; Terns & Dahlberg, 1994), which binds to nucleoporins containing O-linked N-acetylglucosamine residues (Snow et al., 1987). Also, several yeast nucleoporin mutants, which exhibit defects in the nuclear export of polyadenylated RNA, have been identified (reviewed by Rout & Wente, 1994; Davis, 1995; Doye & Hurt, 1995; Panté & Aebi, 1996a). Moreover, at least three yeast nucleoporins (Nup100, Nup116, and Nup145) contain an RNA-binding motif (Fabre et al., 1994; Wente & Blobel, 1994) that binds homopolymeric RNA in vitro (Fabre et al., 1994). Blocking export of all types of RNA-gold conjugate studied here by chilling, or inhibition of U1 ΔSmRNA export by WGA injection, however, did not result in association of the RNA-gold with the nuclear periphery of NPCs.

In previous work it was shown that, in competition experiments between the various classes of RNA stud-

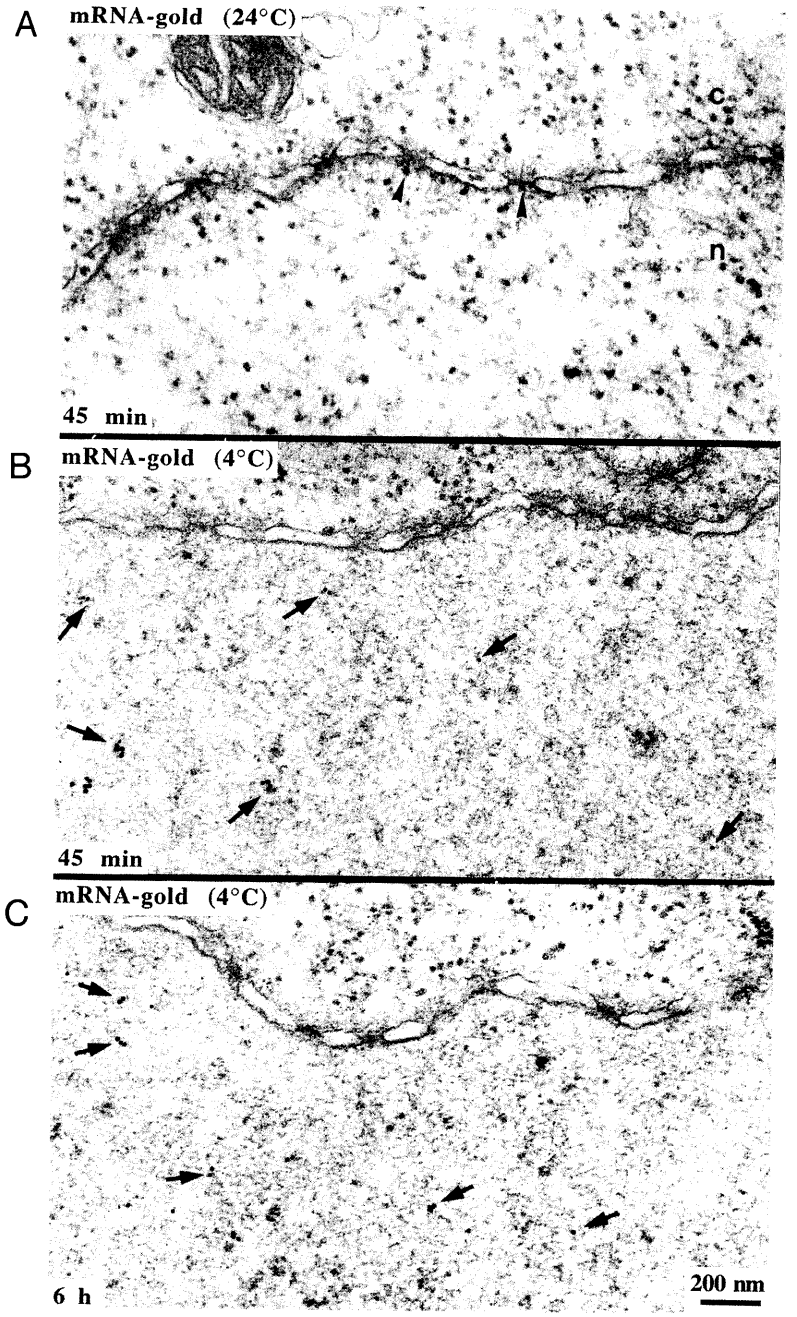

FIGURE 6. Inhibition of nuclear export of DHFR mRNA-gold at low temperature. Shown are cross-sectioned nuclear envelopes from *Xenopus* oocytes that have been microinjected into their nuclei with mRNA-gold and kept at (**A**) room temperature for 45 min, (**B**) 4 °C for 45 min, and (**C**) 4 °C for 6 h after microinjection. Arrowheads in A point to gold particles associated with NPCs, whereas the arrows in B and C point to gold particles that remained in the nucleoplasm when the microinjected oocytes are kept at 4 °C. c, cytoplasmic side of the NE; n, nuclear side of the NE. Scale bar, 200 nm.

ied here, each type of RNA specifically inhibits its own export without affecting the export of the other types of RNA. We confirmed these results by performing competition experiments with RNA–gold complexes and subsequently analyzing the samples by EM. Again, we did not observe targeting of RNA to the NPC in these experiments, but instead, the RNA–gold, even in the presence of a quantity of naked RNA sufficient to saturate limiting export factors, remained dispersed throughout the nucleoplasm. These findings are consistent with the notion that specific factors for each RNA pathway act to mobilize the particular RNA destined for export in the nucleoplasm before association of the export ligand complex with the nuclear periphery of the NPCs. This early step(s) is also prevented by chilling or blocked by the presence of WGA. Cellular factors mediating nuclear import of NLS proteins have been identified recently and characterized molecularly (reviewed by Melchior & Gerace, 1995; Görlich & Mattaj, 1996; Panté & Aebi, 1996b). One of these factors, importin α, is known to shuttle between the cytoplasm and the nucleus. The NH_2-terminal IBB domain of importin α, which is imported similarly to importin α in an importin β-mediated way, acts as a specific inhibitor of importin α-mediated import (Görlich et al., 1996a; Weis et al., 1996) and of U snRNA

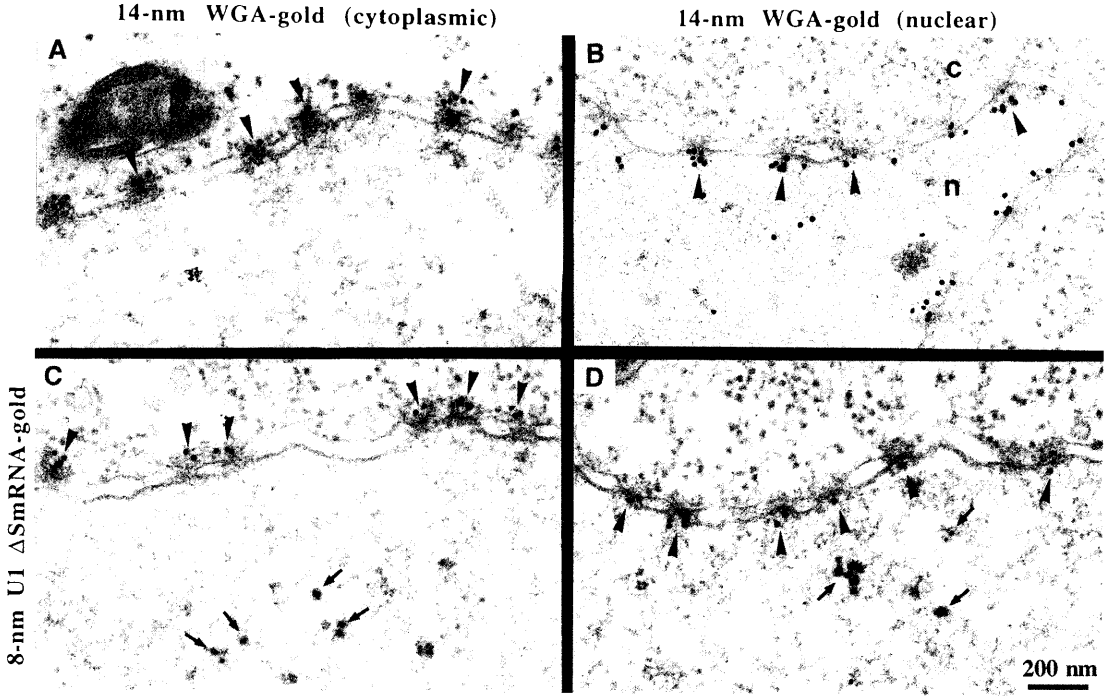

FIGURE 7. Inhibition of nuclear export of U1 ΔSmRNA-gold by cytoplasmic or nuclear microinjection of WGA. Shown are cross-sectioned *Xenopus* oocyte nuclear envelopes from oocytes that have been microinjected with 14-nm WGA-gold into their cytoplasm (**A**) or their nucleus (**B**). At the cytoplasmic side of the NPC, WGA-gold particles were associated with the cytoplasmic periphery of the NPC (A, arrowheads), whereas at the nuclear side of the NPC, WGA-gold particles were found up to a vertical distance of 60 nm from the NPC central plane (B, arrowheads). When 8-nm U1 ΔSmRNA-gold complexes were microinjected into the nucleus of oocytes 1 h after the microinjection of 14-nm WGA-gold into their (**C**) cytoplasm or (**D**) nucleus, the 8-nm gold particles remained in the nucleus (C and D, arrows). c, cytoplasmic side of the NE; n, nuclear side of the NE. Scale bar, 200 nm.

export (Görlich et al., 1996b). By microinjecting this IBB domain into the cytoplasm of *Xenopus* oocytes and analyzing the export of U1 ΔSmRNA-gold, we have shown that importin α specifically inhibited export of this RNA conjugate and caused accumulation in the nucleoplasm rather than at the NPC. Similarly, hnRNP A1, which has been proposed to have a role in the export of mRNA (Piñol-Roma & Dreyfuss, 1992; Michael et al., 1995), was used to saturate the mRNA export pathway specifically (Izaurralde et al., 1997), and again the nonexported mRNA-gold conjugates accumulated throughout the nucleoplasm.

It has been demonstrated previously that low-capacity, nonspecific, RNA binding sites exist within *Xenopus* oocyte nuclei, and that saturation of these sites is required in order to obtain maximal export rates (Pokrywka & Goldfarb, 1995). Because we see no obvious change in the intranuclear distribution of the various types of RNA-gold in the presence of saturating amounts of either specific or nonspecific competitor RNAs, these low-capacity sites cannot be responsible for retaining the RNA-gold complexes in the nucleoplasm in our experiments. The question remains of whether the RNA-gold complexes are freely diffusing within the nucleoplasm, but unable to bind to the NPCs because they lack a specific targeting factor, or are bound to something in the nucleoplasm from which they must be detached before NPC association and export can occur. The rapid dispersal of the RNA-gold particles after their injection seen here and by Dworetzky and Feldherr (1988) is more compatible with the first of these two possible explanations, but does not definitively rule out the second.

In summary, by quantitative EM, we have visualized export intermediates bound to the NPC, at the nuclear basket, and the nuclear and cytoplasmic periphery of the central gated channel. Our attempts to establish experimental conditions yielding accumulation of RNA destined for export at any one of these NPC binding areas have been unsuccessful. These findings indicate that, although nuclear export of RNA and nuclear import of proteins are conceptually similar in that both are targeted vectorial processes mediated by cellular factors and by the NPC, intranuclear steps in RNA export are more significant than intracytoplasmic steps in protein import. Unlike protein import into the nucleus, where stable intermediates accumulate at distinct peripheral NPC sites that are visualized readily by EM (Newmeyer & Forbes, 1988; Richardson et al., 1988; Panté & Aebi, 1996c), no such stable intermediates accumulate at distinct NPC sites during RNA export.

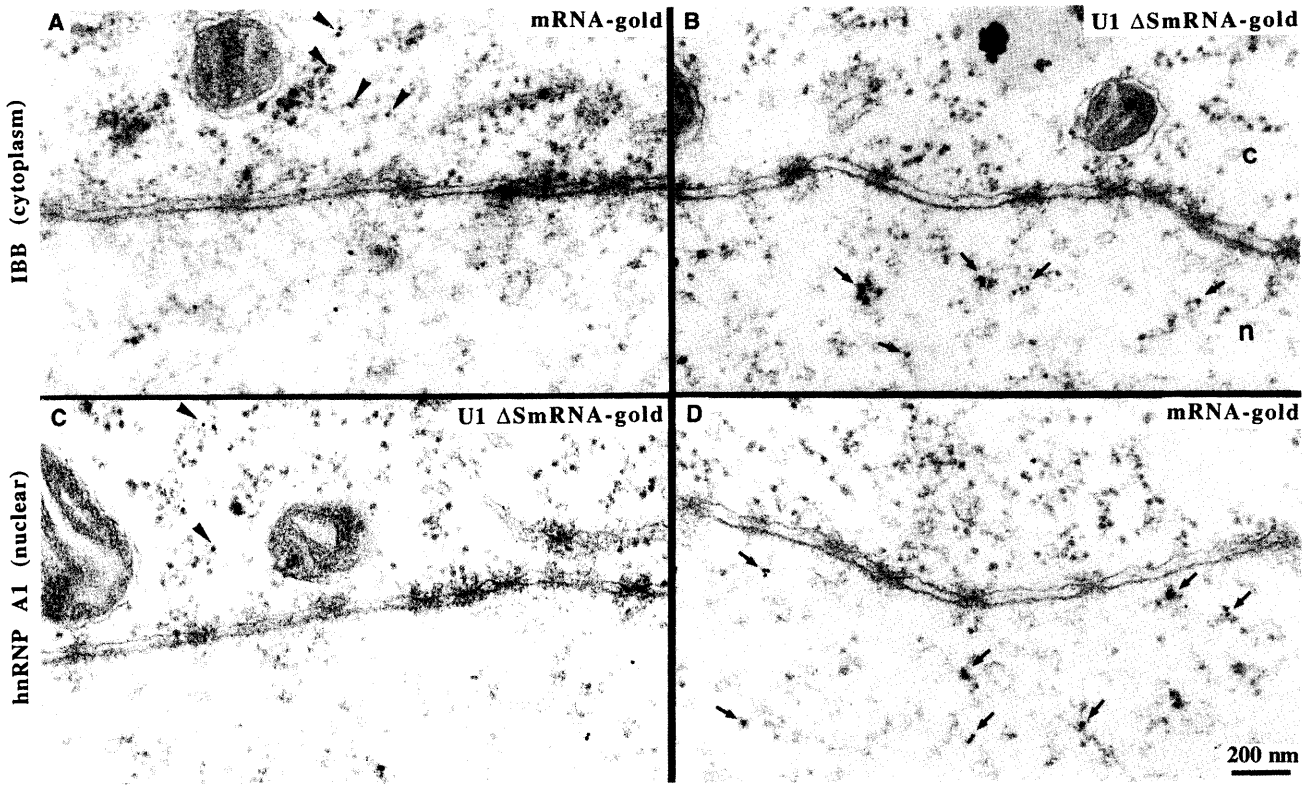

FIGURE 8. Inhibition of the export of U1 ΔSmRNA by the IBB domain and of mRNA by hnRNP A1. Inhibition of nuclear export of U1 ΔSmRNA-gold by cytoplasmic pre-injection of the NH_2-terminal domain of importin α (the IBB domain; Görlich et al., 1996a; Weis et al., 1996). Shown in A and B are cross-sectioned nuclear envelopes from *Xenopus* oocytes that have been microinjected into the cytoplasm with an IBB domain fusion protein 1 h before nuclear microinjection of either (**A**) mRNA-gold or (**B**) U1 ΔSmRNA-gold. The U1 ΔSmRNA-gold particles remained in the nucleoplasm (B, arrows) even after incubation at room temperature for 3 h, whereas mRNA-gold was exported normally. The effect of inhibition of nuclear export of mRNA-gold by nuclear pre-injection of hnRNP A1 are shown in C and D. Cross-sectioned nuclear envelopes from *Xenopus* oocytes that have been microinjected into the nucleus with hnRNP A1 1 h before nuclear microinjection of either (**C**) U1 ΔSmRNA-gold or (**D**) mRNA-gold. The mRNA-gold particles remained in the nucleoplasm (D, arrows) even after incubation at room temperature for 3 h, whereas the U1 ΔSmRNA-gold was exported normally. c, cytoplasmic side of the NE; n, nuclear side of the NE. Scale bar, 200 nm.

MATERIAL AND METHODS

Preparation of RNAs

^{32}P-labeled RNAs were prepared as described previously (Jarmolowski et al., 1994). Large-scale nonradioactive amounts of RNA were prepared using 30 μg of linearized plasmid template and 150 units of T7 RNA polymerase (Promega) according to the instructions of the manufacturer. Trace amounts of [α^{32}P]GTP (20,000–30,000 cpm) were added to enable determination of the concentration of the synthesized RNA. Synthesis of DHFR mRNA and U1 ΔSmRNA was primed with m^7GpppG; synthesis of U6 ΔssRNA, with γmGTP. The concentration of these nucleotides in the transcription reaction was 2.5 mM. Both nucleotides were kindly provide by Edward Darzynkiewicz. Transcription reactions were terminated after 3 h incubation at 37 °C, by addition of 100 units of RNase-free DNase I (Boehringer-Mannheim, Germany). Samples were incubated for an additional hour and then extracted with phenol/chloroform. Unincorporated NTPs were eliminated by a Sephadex G-50 spin column. Ethanol-precipitated RNA was resuspended in water, checked on an 8% denaturing polyacrylamide-7 M urea gel. The concentration was determined using incorporation of [α^{32}P]GTP into RNA. Conjugation to colloidal gold was performed as described below.

Preparation of positive gold colloids

Colloidal gold particles, ~8 nm in diameter, were prepared by reduction of tetrachloroauric acid with sodium citrate in the presence of tannic acid (Slot & Geuze, 1985). These colloidal gold particles are charged negatively. To conjugate them to RNAs, their charge state was reversed by adding $Th(NO_3)_4$. The amount of $Th(NO_3)_4$ required to reverse the charge of the gold colloids was determined for each batch of colloidal gold particles used by mixing 100-μL aliquots of gold colloids with 10 μL of decreasing concentrations of $Th(NO_3)_4$ starting at 0.1 M. In this test, the solution changes from red to blue at higher concentrations of $Th(NO_3)_4$. At lower concentrations of $Th(NO_3)_4$, the solution turns lilac and then red, corresponding to stable, positively charged colloidal gold particles. At even lower concentrations of $Th(NO_3)_4$, the solution turns blue again. Although the amount of $Th(NO_3)_4$ required to reverse the charge of colloidal gold particles changed from batch to batch, we

found that about 5 μL of 2 M $Th(NO_3)_4$ was necessary per milliliter of 8-nm diameter gold colloids.

Direct conjugation of WGA and RNAs with colloidal gold

WGA (Sigma, St. Louis, Missouri) was conjugated to 14-nm diameter colloidal gold particles as described previously (Panté et al., 1994). To conjugate RNA to 8-nm positively charged colloidal gold particles, first the minimal concentration of each RNA required to stabilize the positive colloidal gold particles was determined as follows: 50 μL of positive gold colloids were mixed with 10 μL of various concentrations of RNA, and then the color change of the solution from red to blue was visualized upon addition of 50 μL of 20% ammonium sulfate. The slightest change of color indicated the instability of the RNA–gold complex. The minimal amount of RNA required to stabilize the colloidal gold particles was the minimal concentration at which the solution did not change color. The amount of RNA per milliliter of 8-nm diameter positively charged colloidal gold was: 5–10 μg for DHFR-mRNA, 2–8 μg for tRNA, and 1–4 μg for U1 ΔSmRNA. RNA–gold complexes were then formed by mixing the RNA and positively charged colloidal gold particles for 10 min at room temperature. The complexes were centrifuged at 45,000 × *g* for 15 min, the pellet was resuspended in low-salt buffer (LSB) containing 1 mM KCl, 0.5 mM $MgCl_2$, 10 mM Hepes, pH 7.5, and used immediately for microinjection. For some experiments, [^{32}P]RNAs were conjugated to 8-nm colloidal gold by the same method.

To confirm that the RNA was conjugated to colloidal gold particles, the RNA–gold complex was destabilized by freezing in liquid nitrogen. This procedure dissociated the gold particles from the RNA. After thawing, the sample was then centrifuged in an Eppendorf centrifuge, and the supernatant was checked for the presence of RNA with ethidium bromide under a UV source.

Oocyte microinjection

Mature (stage six) oocytes were surgically removed from female *Xenopus laevis* as described previously (Reichelt et al., 1990; Jarnik & Aebi, 1991), and stored in modified Barth's saline (MBS) containing 88 mM NaCl, 1 mM KCl, 0.82 mM $MgSO_4$, 0.33 mM $Ca(NO_3)_2$, 0.41 mM $CaCl_2$, 10 mM Hepes, pH 7.5. Oocytes were defolliculated by treatment with 5 mg/mL collagenase (Sigma, St. Louis, Missouri) in calcium-free MBS for 3 h. Oocytes were then washed with MBS and used for microinjection within the next two days. To visualize the oocyte nuclei for nuclear injections, the oocytes were centrifuged at 2,000 × *g* for 10 min at 4 °C, as described previously (Hamm & Mattaj, 1990). About 20 nL of RNA (gold-conjugated or ^{32}P-labeled, see below) was microinjected into the nucleus of each oocyte. The injected oocytes were incubated in MBS buffer at room temperature for the indicated times and analyzed by EM as described below.

For inhibition of nuclear export by chilling, oocytes were cooled to 4 °C 30 min before microinjection of gold-labeled RNAs, and were then kept at this temperature for 6 h after injection. For WGA inhibition, 50 nL of WGA at 20 mg/mL was microinjected into the oocyte cytoplasm (or 20 nL at 5 mg/mL for nuclear injections), and the oocytes were incubated at room temperature for 1 h before the nuclear injection of gold-labeled RNAs. As indicated, in some experiments, 14-nm diameter gold-conjugated WGA was used.

For competition experiments, unlabeled RNAs were microinjected into the nuclei of *Xenopus* oocytes 1 h before the nuclear microinjection of RNA–gold complexes at concentrations sufficient to cause saturation (Jarmolowski et al., 1994), and samples were incubated at room temperature for the indicated times. The recombinant IBB domain (amino acids 1–55 of *Xenopus* importin α fused to the IgG binding z domain of protein A; Görlich et al., 1996b) at 10 mg/mL or hnRNP A1 at 4 mg/mL were injected into the cytoplasm or nucleus, respectively, 1 h before nuclear injection of the RNA–gold conjugates.

Quantitation of nuclear export

To quantify the export of gold-labeled RNAs, oocytes were microinjected with gold-conjugated [^{32}P]RNAs. After incubation at 19 °C for various times, nuclei were manually dissected and the radioactivity in the nuclear and cytoplasmic fractions was determined by counting in a scintillation counter.

Preparation of samples for electron microscopy

For EM, oocyte nuclei were microinjected with gold-conjugated RNAs. After incubation at room temperature for the indicated times, injected oocytes were fixed overnight at 4 °C in MBS (see above) containing 2% glutaraldehyde. The oocytes were then washed three times with MBS, and the nuclei (with the remaining surrounding cytoplasm) were dissected and fixed again with 2% glutaraldehyde in LSB (see above) for 1 h at 4 °C. Samples were washed three times with LSB, and post-fixed for 1 h with 1% OsO_4 in LSB. Next, the chemically fixed samples were dehydrated and embedded in Epon 812 resin by conventional procedures (Jarnik & Aebi, 1991). Thin sections were cut on a Reichert Ultracut ultramicrotome (Reichert-Jung Optische Werke, Vienna, Austria) using a diamond knife. The sections were collected on carbon/colloidon-coated EM grids, stained with 6% uranyl acetate for 45 min, and post-stained with lead citrate for 1 min (Milloning, 1961). Micrographs were recorded with a Hitachi H-8000 transmission electron microscope (Hitachi Ltd., Tokyo, Japan) operated at an acceleration voltage of 75 kV.

ACKNOWLEDGMENTS

We thank Dr. D. Görlich for the kind gift of recombinant IBB fusion protein, Dr. M. Döbeli for help with the data analysis, Ms. H. Frefel and Ms. M. Zoller for their expert photographic work. This work was supported by the Kanton Basel-Stadt, the M.E. Müller Foundation of Switzerland, and by research grants from the Swiss National Science Foundation (31-39691.93), the Polish Research Committee (KBN 6P04A03511) and the Human Frontier Science Program Organization. E.I. was a recipient of a fellowship from the Human Frontier Science Program Organization.

Received December 20, 1996; returned for revision February 5, 1997; revised manuscript received February 18, 1997

REFERENCES

Akey CW, Radermacher M. 1993. Architecture of the *Xenopus* nuclear pore complex revealed by three-dimensional cryo-electron microscopy. *J Cell Biol 122*:1-19.

Bataillé N, Helser T, Fried HM. 1990. Cytoplasmic transport of ribosomal subunits microinjected into the *Xenopus laevis* oocyte nucleus: A generalized, facilitated process. *J Cell Biol 111*:1571-1582.

Bogerd HP, Fridell RA, Madore S, Cullen BR. 1995. Identification of a novel cellular cofactor for the Rev/Rex class of retroviral regulatory proteins. *Cell 82*:485-494.

Bogerd HP, Fridell RA, Benson RE, Hua J, Cullen BR. 1996. Protein sequence requirements for function of the human T-cell leukemia virus type 1 rex nuclear export signal delineated by a novel in vivo randomization-selection assay. *Mol Cell Biol 16*:4207-4214.

Boulikas T. 1993. Nuclear localization signals (NLS). *Crit Rev Eukar Gene Expr 3*:193-227.

Davis LI. 1995. The nuclear pore complex. *Annu Rev Biochem 64*:865-896.

Dingwall C, Laskey RA. 1991. Nuclear targeting sequences—A consensus? *Trends Biochem Sci 16*:478-481.

Doye V, Hurt EC. 1995. Genetic approaches to nuclear pore structure and function. *Trends Genet 11*:235-241.

Duverger E, Pellerin-Mendes C, Mayer R, Roche AC, Monsigny M. 1995. Nuclear import of glycoconjugates is distinct from the classical NLS pathway. *J Cell Sci 108*:1325-1332.

Dworetzky S, Feldherr CM. 1988. Translocation of RNA-coated gold particles through the nuclear pores of oocytes. *J Cell Biol 106*:575-584.

Fabre E, Boelens WC, Wimmer C, Mattaj IW, Hurt EC. 1994. Nup145p is required for nuclear export of mRNA and binds homopolymeric RNA in vitro via a novel conserved motif. *Cell 78*:275-289.

Featherstone C, Darby MK, Gerace L. 1988. A monoclonal antibody against the nuclear pore complex inhibits nucleocytoplasmic transport of protein and RNA in vivo. *J Cell Biol 107*:1289-1297.

Fischer U, Meyer S, Teufel M, Heckel C, Lührmann R, Rautmann G. 1994. Evidence tht HIV-1 Rev directly promotes the nuclear export of unspliced RNA. *EMBO J 13*:4105-4112.

Fischer U, Huber J, Boelens WC, Mattaj IW, Lührmann R. 1995. The HIV-1 Rev activation domain is a nuclear export signal that accesses an export pathway used by specific cellular RNAs. *Cell 82*:475-483.

Fischer U, Michael WM, Lührmann R, Dreyfuss G. 1996. Signal-mediated nuclear export pathways of proteins and RNAs. *Trends in Cell Biol 6*:290-293.

Fridell RA, Fischer U, Lührmann R, Meyer BE, Meinkoth JL, Malim MH, Cullen BR. 1996. Amphibian transcription factor IIIA proteins contain a sequence element functionally equivalent to the nuclear export signal of human immunodeficiency virus type 1 Rev. *Proc Natl Acad Sci USA 93*:2936-2940.

Fritz CC, Green MR. 1996. Hiv Rev uses a conserved cellular protein export pathway for the nucleocytoplasmic transport of viral RNAs. *Curr Biol 6*:848-854.

Fritz CC, Zapp ML, Green MR. 1995. A human nucleoporin-like protein that specifically interacts with HIV Rev. *Nature 376*:530-533.

Garcia-Bustos J, Heitman J, Hall MN. 1991. Nuclear protein localization. *Biochim Biophys Acta 1071 B*:83-101.

Gerace L. 1995. Nuclear export signals and the fast track to the cytoplasm. *Cell 82*:341-344.

Görlich D, Henklein P, Laskey RA, Hartmann E. 1996a. A 41 amino acid motif in importin-α confers binding to importin-β and hence transit into the nucleus. *EMBO J 15*:1810-1817.

Görlich D, Kraft R, Kostka S, Vogel F, Hartmann E, Laskey RA, Mattaj IW, Izaurralde E. 1996b. Importin provides a link between nuclear protein import and U snRNA export. *Cell 87*:21-32.

Görlich D, Mattaj IW. 1996. Nucleocytoplasmic transport. *Science 271*:1513-1518.

Görlich D, Panté N, Kutay U, Aebi U, Bischoff FR. 1996c. Identification of different roles for Ran GDP and Ran GTP in nuclear protein import. *EMBO J 15*:5584-5594.

Guddat U, Bakken AH, Pieler T. 1990. Protein-mediated nuclear export of RNA: 5S rRNA containing small RNPs in *Xenopus* oocytes. *Cell 60*:619-628.

Hamm J, Mattaj IW. 1990. Monomethylated cap structures facilitate RNA export from the nucleus. *Cell 63*:109-118.

Hinshaw JE, Carragher BO, Milligan RA. 1992. Architecture and design of the nuclear pore complex. *Cell 69*:1133-1141.

Izaurralde E, Jarmolowski A, Beisel C, Mattaj IW, Dreyfuss G, Fischer U. 1997. A role for the hnRNPA1 M9-transport signal in mRNA nuclear export. *J Cell Biol*. Forthcoming.

Izaurralde E, Lewis J, Gamberi C, Jarmolowski A, McGuigan C, Mattaj IW. 1995. A cap-binding protein complex mediating U snRNA export. *Nature 376*:709-712.

Izaurralde E, Lewis J, McGuigan C, Jankowska M, Darzynkiewicz E, Mattaj IW. 1994. A nuclear cap-binding protein complex involved in pre-mRNA splicing. *Cell 78*:657-668.

Izaurralde E, Mattaj IW. 1992. Transport of RNA between nucleus and cytoplasm. *Semin Cell Biol 3*:279-288.

Izaurralde E, Mattaj IW. 1995. RNA export. *Cell 81*:153-159.

Izaurralde E, Stepinski J, Darzynkiewicz E, Mattaj IW. 1992. A cap binding protein that may mediate nuclear export of RNA polymerase II-transcribed RNAs. *J Cell Biol 118*:1287-1295.

Jarmolowski A, Boelens WC, Izaurralde E, Mattaj IW. 1994. Nuclear export of different classes of RNA is mediated by specific factors. *J Cell Biol 124*:627-635.

Jarnik M, Aebi U. 1991. Toward a more complete 3-D structure of the nuclear pore complex. *J Struct Biol 107*:291-308.

Kiseleva E, Goldberg MW, Daneholt B, Allen TD. 1996. RNP export is mediated by structural reorganization of the nuclear pore basket. *J Mol Biol 260*:304-311.

Koepp DM, Silver PA. 1996. A GTPase controlling nuclear trafficking: Running the right way or walking RANdomly? *Cell 87*:1-4.

Lührmann R, Kastner B, Bach M. 1990. Structure of spliceosomal snRNPs and their role in pre-mRNA splicing. *Biochim Biophys Acta 1087*:265-292.

Malim MH, Cullenv BR. 1993. Rev and the fate of pre-mRNA in the nucleus: Implications for the regulation of RNA processing in eukaryotes. *Mol Cell Biol 13*:6180-6189.

Mehlin H, Daneholt B, Skoglund U. 1992. Translocation of a specific premessenger ribonucleoprotein particle through the nuclear pore studied with electron microscope tomography. *Cell 69*:605-613.

Mehlin H, Daneholt B, Skoglund U. 1995. Structural interaction between the nuclear pore complex and a specific translocating RNP particle. *J Cell Biol 129*:1205-1216.

Melchior F, Gerace G. 1995. Mechanism of nuclear protein import. *Curr Opin Cell Biol 7*:310-318.

Michael WM, Choi M, Dreyfuss G. 1995. A nuclear export signal in hnRNP A1: A signal-mediated, temperature-dependent nuclear protein export pathway. *Cell 83*:415-422.

Milloning G. 1961. A modified procedure for lead staining of thin sections. *J Biophys Biochem Cytol 11*:736-739.

Neuman de Vegvar HE, Dahlberg JE. 1990. Nucleocytoplasmic transport and processing of small nuclear RNA precursors. *Mol Cell Biol 10*:3365-3375.

Newmeyer DD, Forbes DJ. 1988. Nuclear import can be separated into distinct steps in vitro: Nuclear pore binding and translocation. *Cell 52*:641-653.

Panté N, Aebi U. 1996a. Molecular dissection of the nuclear pore complex. *CRC Critical Rev Biochem Mol Biol 31*:153-199.

Panté N, Aebi U. 1996b. Signal pathways for nuclear import and export. *Curr Opin Cell Biol 8*:397-406.

Panté N, Aebi U. 1996c. Sequential binding of import ligands to distinct nucleopore regions during their nuclear import. *Science 273*:1729-1733.

Panté N, Bastos R, McMorrow I, Burke B, Aebi U. 1994. Interactions and three-dimensional localization of a group of nuclear complex proteins. *J Cell Biol 126*:603-617.

Piñol-Roma S, Dreyfuss G. 1992. Shuttling of pre-mRNA binding proteins between nucleus and cytoplasm. *Nature 355*:730-732.

Pokrywka NJ, Goldfarb DS. 1995. Nuclear export pathways of tRNA and 40 S ribosomes include both common and specific intermediates. *J Biol Chem 270*:3619-3624.

Pollard VW, Michael WM, Nakielny S, Siomi MC, Wang F, Dreyfuss G. 1996. A novel receptor-mediated nuclear protein import pathway. *Cell 86*:985–994.

Reichelt R, Holzenburg A, Buhle EL, Jarnik M, Engel A, Aebi U. 1990. Correlation between structure and mass distribution of the nuclear pore complex, of distinct pore complex components. *J Cell Biol 110*:883–894.

Richardson WD, Mills AD, Dilworth SM, Laskey RA, Dingwall C. 1988. Nuclear protein migration involves two steps: Rapid binding at the nuclear envelope followed by slower translocation through the nuclear pores. *Cell 52*:655–664.

Rout M, Wente SR. 1994. Pores for thought: Nuclear pore complex proteins. *Trends Cell Biol 4*:357–365.

Siomi H, Dreyfuss G. 1995. A nuclear localization domain in the hnRNP A1 protein. *J Cell Biol 129*:551–559.

Slot JW, Geuze HJ. 1985. A new method of preparing gold probes for multiple-labeling cytochemistry. *Eur J Cell Biol 38*:87–93.

Snow CM, Senior A, Gerace L. 1987. Monoclonal antibodies identify a group of nuclear pore complex glycoproteins. *J Cell Biol 104*:1143–1156.

Stutz F, Izaurralde E, Mattaj IW, Rosbash M. 1996. A role for nucleoporin FG-repeat domains in HIV-1 Rev protein and RNA export from the nucleus. *Mol Cell Biol 16*:7144–7150.

Stutz F, Neville M, Rosbash M. 1995. Identification of a novel nuclear pore-associated protein as a functional target of the HIV-1 Rev protein in yeast. *Cell 82*:495–506.

Terns MP, Dahlberg JE. 1994. Retention and 5′ cap trimethylation of U3 snRNA in the nucleus. *Science 264*:959–961.

Vankan P, McGuigan C, Mattaj IW. 1990. Domains of U4 and U6 snRNAs required for snRNP assembly and splicing complementation in *Xenopus* oocytes. *EMBO J 9*:3397–3404.

Verkleij AJ, Leunissen JLM. 1990. Immuno-gold labeling in cell biology. Boca Raton, Florida: CRC Press, Inc.

Visa N, Alzhanova-Ericsson AT, Sun X, Kiseleva E, Bjorkroth B, Wurtz T, Daneholt B. 1996a. A pre-mRNA-binding protein accompanies the RNA from the gene through the nuclear pores and into polysomes. *Cell 84*:253–264.

Visa N, Izaurralde E, Ferreira J, Daneholt B, Mattaj IW. 1996b. A nuclear cap-binding complex binds balbiani ring pre-mRNA cotranscriptionally and accompanies the ribonucleoprotein particle during nuclear export. *J Cell Biol 133*:5–14.

Weighardt F, Biamonti G, Riva S. 1995. Nucleo-cytoplasmic distribution of human hnRNP proteins: A search for the targeting domains in hnRNP A1. *J Cell Sci 108*:545–555.

Weis K, Ryder U, Lamond AI. 1996. The conserved amino-terminal domain of hSRP1α is essential for nuclear protein import. *EMBO J 15*:1801–1809.

Wen W, Meinkoth JL, Tsien RY, Taylor SS. 1995. Identification of a signal for rapid export of proteins from the nucleus. *Cell 82*:463–473.

Wente SR, Blobel G. 1994. *NUP145* encodes a novel yeast glycine-leucine-phenylalanine-clycine (GLFG) nucleoporin required for nuclear envelope structure. *J Cell Biol 125*:955–969.

Zasloff M. 1983. tRNA transport from the nucleus in a eukaryotic cell: Carrier-mediated translocation process. *Proc Natl Acad Sci USA 80*:6436–6440.